MONODISPERSE COLLOIDAL SUSPENSIONS OF SILICA AND PMMA SPHERES AS MODEL ELECTRORHEOLOGICAL FLUIDS: A REAL-SPACE STUDY OF STRUCTURE FORMATION

ANAND YETHIRAJ AND ALFONS VAN BLAADEREN

Soft Condensed Matter, Utrecht University, and FOM Institute for Atomic and Molecular Physics, Amsterdam, The Netherlands. Email: yethiraj@amolf.nl, A.vanBlaaderen@phys.uu.nl

Colloidal particle coordinates in three dimensions can be obtained in 3D samples with a combination of the increased resolution and optical sectioning capabilities of confocal microscopy and fluorescently labeled model core-shell silica colloids. In this work we show how this capability can be used to analyze structure formation in electrorheological fluids on a quantitative basis. We find body-centered-tetragonal (BCT) crystals for colloidal particles in an electric field. Metastable sheet like structures were identified as an intermediate phase prior to BCT crystal formation. Due to finite-size effects induced by the electrode surface the sheets are not randomly oriented, but grow preferentially with a 60^{o} tilt with respect to the electric field. Preliminary measurements indicate that flow-aligned sheets form under shear. Finally, we show that in the case that the ionic strength is very low, electric-field-induced dipolar interactions can be present in addition to long-range repulsions between the colloids leading to interesting metastable and equilibrium structures with possibilities for applications in photonic bandgap crystals as well as in model ER studies.

1 Introduction

Electrorheological (ER) [1] and magnetorheological (MR) fluids have been studied since the 1950's with a view to developing wide-ranging applications that relate to the reversible millisecond field-responsive control of the apparent fluid viscosity. Commercial ER and MR fluids are "messy" systems of odd-shaped and polydisperse sub-millimeter particles in a fluid suspension. The detailed physical mechanisms and the role of variables such as size and shape polydispersity, the role of a mobile surface-charge layer in the ER case, and the role of Brownian motion, are only now beginning to be understood (see [2] for a recent review). Moreover, while rheological measurements have yielded a lot of information, there is yet only limited information about the kinds of structures formed [3-5] and their dynamics. In this paper, we describe a technique and two model systems for studying the kinetics of the ER response.

2 Methods

Two model ER fluids are used in our studies. The first is a suspension of monodisperse 1.4 μm silica spheres, where the spheres have a fluorescent-labeled core surrounded by a non-fluorescent shell [6]. The solvent is a

mixture of water and glycerol, with 16% water by weight, in order to match the refractive index of the silica spheres, enabling imaging in the single-scattering limit. The inter-particle interactions here are known to be hard-sphere like in the absence of the field. The second system is a suspension of 2 μm polymethyl methacrylate (PMMA) fluorescent spheres [7], sterically stabilized with a poly-hydroxysteric acid (PHSA) surface coating, in an organic solvent (a mixture of cyclo-heptyl bromide and cis-decalin, where simultaneous matching of refractive-index and density to that of PMMA is possible) where the inter-particle interactions are soft due to the combination of charge on the sphere surface and a large Debye length in the solvent. Images are obtained via fluorescent confocal laser scanning microscopy, three-dimensional structure information (see Ref. [8] for details) of a sample volume of 100 μm x 100 μm x 50 μm in several seconds, and two-dimensional structure information in a sample area of 100 μm x 100 μm on the timescale of a second.

The field is varied up to E_{peak} =1 V /μm (E_{rms} = 0.707*E_{peak}) in the silica system and 2 V/μm in the PMMA system, while the frequency is maintained at 1 MHz to be well above the low-frequency electrohydrodynamic effects associated with the double layer. The applied field is monitored with an oscilloscope. The electrode gap is maintained at about 100 μm. While the silica spheres and the solvent are index-matched at light frequencies, the dielectric constant mismatch at 1MHz is still essentially the same as at zero frequency and enough to explain the strong ER effect. In the PMMA suspension, the zero-frequency dielectric mismatch is an order of magnitude lower, and the mechanism for the relatively strong ER response reported here is as yet unknown.

3 Results

3.1 The ER Effect in The Hard-Sphere System: Strings, Two-Strings, Sheets and BCT Crystallites.

In the silica/water-glycerol system, we observe the almost instantaneous formation of strings (timescale ~ milliseconds) and the subsequent slower formation of sheets and BCT crystals (with the shortest interparticle spacing in the c direction and a:c≡ b:c=.√3/√2; first predicted as a minimum energy structure in Ref. 9). This has been reported in an earlier work [5]. Time scales associated with the aggregation of columns is expected [10] to be on the order of $\tau \sim (\eta/k_BT)\ r_\perp^3$ ~ 15 sec. for single-

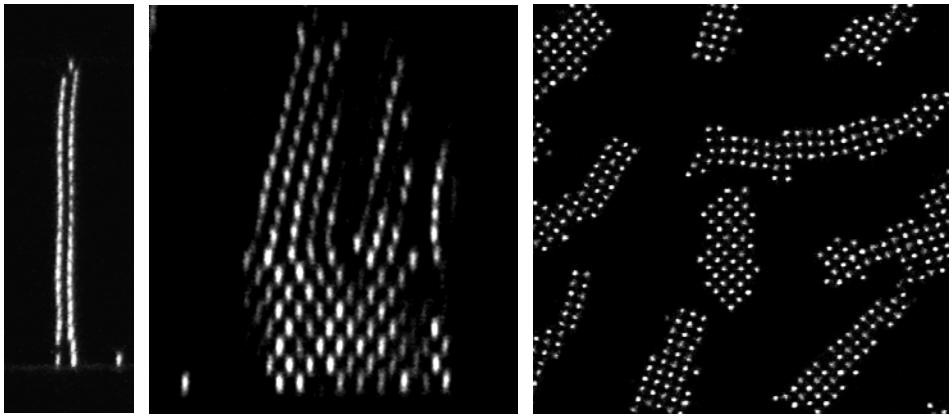

Figure 1(a) x-z of two-string (b) x-z of sheets in tilt transition (c) x-y of BCT crystallites. Particle volume fraction $\varphi \approx 15\%$; E_{peak} =1 V /μm.

chain columns of 1.4 μm diameter spheres, given the 230 mPa.s viscosity of the index-matched water-glycerol mixture. The sedimentation rate of silica spheres in the viscous solvent mixture is on the order of μm/minute. This is consistent with the calculated sedimentation velocity $v = mg/\gamma_0 = (0.1 \times 10^{-12})/(5 \times 10^{-6}) \sim 0.02$ μm/sec, where $\gamma_0 = 6\pi\eta R$ is the viscous drag coefficient.

Unless specifically stated, all images shown in this work are XY slices in the mid-plane of the sample, perpendicular to the applied electric field (along Z). Thus, a string appears as a single particle, a sheet looks like a chain of particles, and the BCT structure looks like two interpenetrating square lattices of more-in-focus and less-in-focus spheres. The formation of sheets is particularly interesting. First a string attracts a neighbor to form a two-string. Two-strings are typically not vertical but slightly bent near the top electrode (see Figure 1a). The two-strings further coarsen to form sheets. As reported in Ref. 5, the sheets are composed of 60°-tilted strings. This effect arises from the fact that while the bulk dipolar interaction is insensitive to the angle of the hexagonal sheet with respect to the field direction, the tilted sheets are energetically favorable due to boundary effects. In fact, we see a transition from vertical strings, to sheets composed of tilted strings and finally to a BCT structure (Fig. 1c) composed of vertical strings. Fig. 1(b) captures this tilt transition.

3.2 Coarsening of Structures: The Time-Evolution in the Formation of the BCT crystallites

The time evolution of the structures is shown in two-dimensional snapshots in Fig. 2, all taken in a plane perpendicular to the field direction.

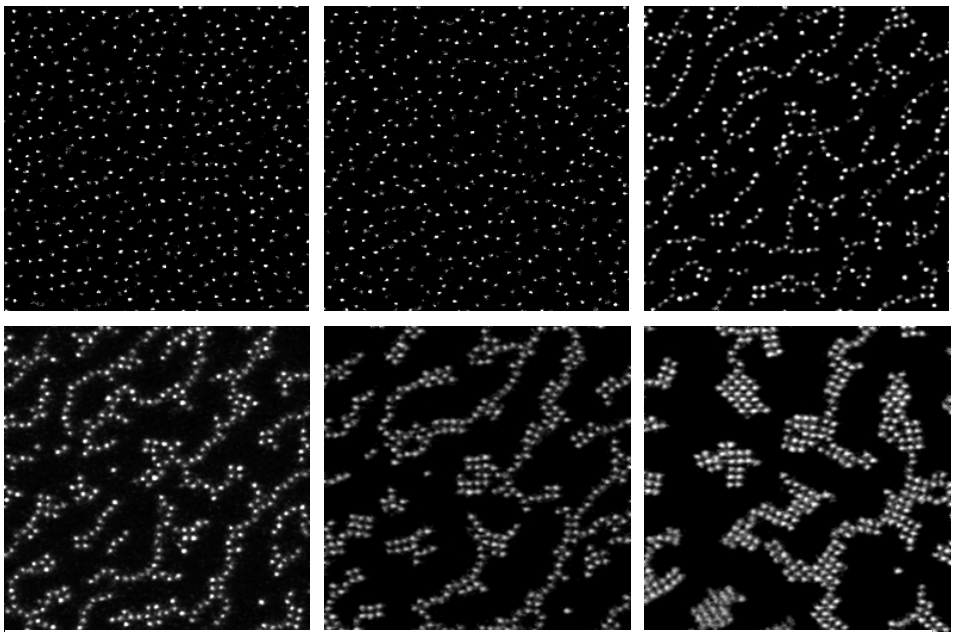

Figure 2 Coarsening of structures beginning from (a) t=0s, (b) t=10 s, (c) t=100s, (d) t=400s, (e) t=2400, f) t=36000s. The coarsening diplays an evolution from strings to sheets to a network of BCT (body-centred cubic) crystallites. $\varphi \approx 15\%$, $E_{peak} = 1V/\mu m$.

The time sequence shows snapshots taken at t=0 s, 1s, 100s, 400s, 2400s, 36000s, respectively. Sheet formation has already begun in Fig. 2(b), while a few small BCT crystallites can be in seen in Fig 2(c) in the form of right-angle kinks in the meandering sheet structure. Further structure formation is extremely slow, and the structure at 36000 s (10 hours) is not significantly different from that at 180000 s (~3 days). In fact, because there is no further significant time-evolution between 10 hours and 3 days, the data therein may be used to study fluctuations in the final structure, which is a network of three-dimensional BCT crystallites. A pictorial

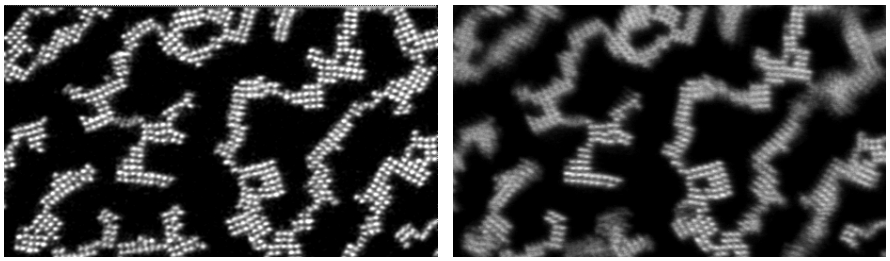

Figure 3 (a) Snapshot of the end state of coarsening observed over three days. (b) An average of the time series of 90 frames once coarsening is too slow to observe exhibits that the large crystallites fluctuate very little, while the single sheets fluctuate the most. $\varphi \approx 15\%$,; $E_{peak} = 1$ V /μm.

representation of this is provided in Fig. 3. Fig 3(a) is a snapshot of the final structure, while Fig. 3(b) is an average from a time series of 87 frames. If a string (seen in the xy image as a sphere) moves little during these frames its average image is not much different from that in a snapshot. However, if its position fluctuates the corresponding region in the average image is blurred. Comparing Fig. 3(a) and 3(b) we notice that the thick columns fluctuate the least (are sharpest defined in the average image) while the single sheets are the most blurred. In order for a structure to evolve, it must sample the space of possible structures, and thus it will take a long time (weeks!) for the small 5-particle-wide BCT crystallites to coarsen further.

3.3 Tuning interactions: ER Effect in the Soft Sphere System

Suspensions of PMMA spheres in the refractive-index and density-matched solvent-mixture of cyclo-heptyl bromide and decalin exhibit a surprisingly strong ER response. At 1 V/μm, the system forms strings that completely span the electrodes (Fig. 4(a)). In contrast with the "hard-

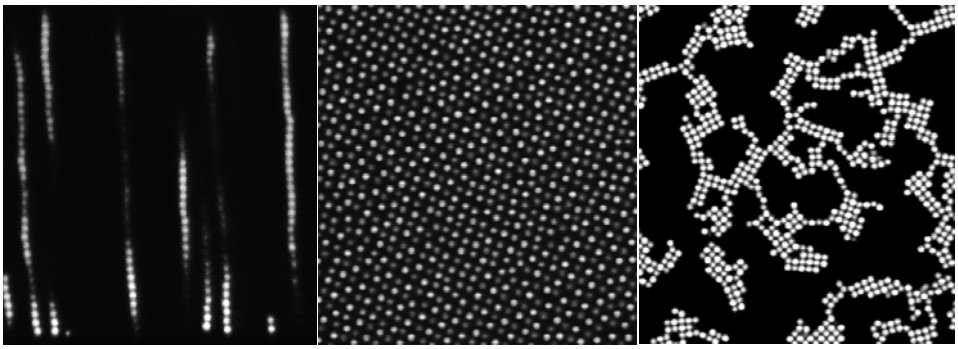

Figure 4 (a) String formation; $\varphi \approx 10\%$, $E_{peak} = 1$V/μm (XZ snapshot) (b) A space-filling tetragonal crystal; $\varphi \approx 25\%$, $E_{peak} = 1$V/μm. (c) Network of BCT crystallites; $\varphi \approx 25\%$, $E_{peak} = 2$ V/μm.

sphere" system reported above, and in Ref. 5, these strings in this field regime are stable, and do not in time agglomerate to form sheets. As the concentration is increased the strings that form do eventually order in a quasi-two-dimensional fashion (the third dimension already being ordered by the formation of strings) to form space-filling crystals, such as the tetragonal crystal shown in Fig 4(b). This is different from the BCT crystals reported earlier in that these crystals do not have the ratio a:c≡ b:c=.√3/√2. *Instead this ratio is determined purely by the constraint of filling space.* The likely reason for this is that charge repulsion of the spheres at low fields is still strong compared to the dipolar interaction. As the field is increased, the dipolar interaction first wins along the field

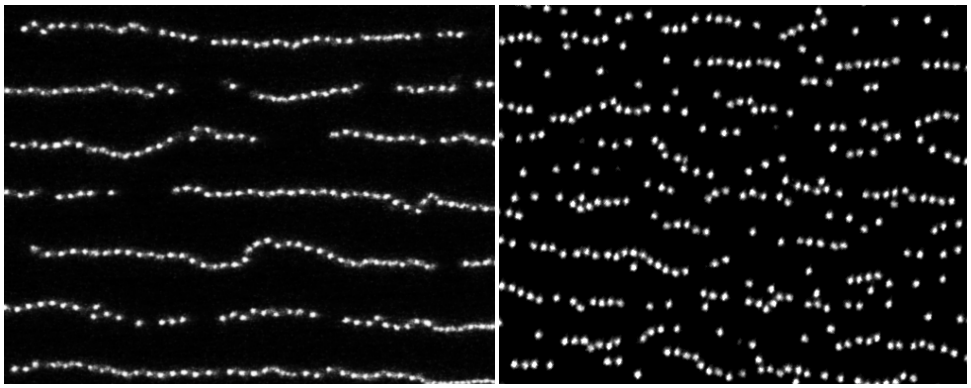

Figure 5 Sheets after shear (a) aqueous silica system (b) non-aqueous PMMA system. $E_{peak} = 1V/\mu m$.

direction, but due to its anisotropic nature, there is a range of field values where the soft repulsion dominates in the plane perpendicular to the field. At a higher field of ~ 2 V/μm, these space-filling structures eventually give way to the expected BCT crystallites characteristic of the dipole-interaction dominated regime (Fig. 4(c)). The BCT crystallites seen here are very similar to the ones observed in the aqueous silica suspensions.

3.4 The Effect of Shear

Next, we explore the effect of shear. Preliminary experiments reveal a qualitative feature of shear: the lining up of sheets along the shear field. There also appears to be a characteristic spacing between sheets that appears at the onset of shear. This is seen in both model systems (Fig. 5). The spacing in both cases is set simply by the particle volume fraction, or when seen in a two-dimensional snapshot (the third dimension being irrelevant because the sheets span the entire region between the electrodes), the particle area fraction which in turn determines the number of particles in focus un the field of view. The applied shear aligns the sheets along the shear direction. The total number of sheets (and hence the spacing) is simply set by the total number of particles in the field of view.

4 Discussion and Conclusions

We have explored two systems in this study, both versatile systems for studying ER mechanisms. The first is in zero field a suspension of hard spheres. This system behaves much like commercial ER fluids, except that the appreciable size polydispersity in the latter likely prevents the formation of the three-dimensional BCT crystal. Here we observe the transition from strings to two-strings, sheets (with strings tilted 60°), double-sheets, and finally crystallites of the BCT structure, which coarsen

extremely slowly in time. The second system, which in zero field is a charged suspension with soft, repulsive interactions, exhibits a novel intermediate-field regime where the strings remain individual strings and do not agglomerate into sheets, as well as new crystal structures that are of interest too in engineering photonic band gap crystals [11], and in the more pedagogical study of a martensitic crystal-to-crystal transition. At high fields, this system also exhibits the string-to-sheet-to-BCT coarsening, establishing qualitatively similar structure formation.

Acknowledgements

We acknowledge Hans Wisman (electronics), Jacob Hoogenboom and Gilles Bosma (silica and PMMA particle synthesis respectively). This work was supported by the Stichting voor Fundamenteel Onderzoek der Materie (FOM), which is part of the Nederlandse Organisatie voor Wetenschappelijk Onderzoek (NWO).

References

1. Winslow W. M., *J. Appl. Phys.* **20**, 1138 (1949).
2. Parthasarathy M and Klingenberg D, *Mater. Sci. Eng.* R. **17**, 57 (1996).
3. Martin J. E., Anderson R. A., and Tigges C. P., *J. Chem. Phys.* **108**, 3765 (1998).
4. Martin J. E., Anderson R. A., and Tigges C. P., *J. Chem. Phys.* **110**, 4854 (1999).
5. Dassanayake U., Fraden S., and van Blaaderen A., *J. Chem. Phys.* **112**, 3851 (2000).
6. van Blaaderen A. and Vrij A., *Langmuir* **8**, 2921 (1992).
7. Bosma G., Pathmamanoharan C., de Hoog E. H. A., Kegel W. K., van Blaaderen A., Lekkerkerker H. N. W., *Langmuir*, accepted for publication; de Hoog E. H. A., Kegel W. K., van Blaaderen A, Lekkerkerker H. N. W., *Phys. Rev. E.* **64,** 1407 (2001).
8. van Blaaderen A.and Wiltzius P., *Science* **270**, 1177 (1995).
9. Tao R. and Sun J. M., *Phys. Rev. Lett.* **68**, 2555 (1992).
10. Halsey T. C. and Toor W., *Phys. Rev. Lett.* **65**, 2820 (1990).
11. van Blaaderen A., Velikov K. P., Hoogenboom J. P., Vossen D. L. J., Yethiraj A., Dullens R., van Dillen T., and Polman A., In: C.M. Soukoulis (ed.), "Photonic Crystals and Light Localization in the 21st Century ", pp.239-251 (Kluwer Academic, Dordrecht, 2001).